Title	Off-center rattling and thermoelectric properties of type-II clathrate (K, Ba)(24)(Ga, Sn, square)(136) single crystals
Auther(s)	Mano, Satomi; Onimaru, Takahiro; Yamanaka, Shoji; Takabatake, Toshiro
Citation	Physical Review B , 84 (21) : 214101
Issue Date	2011
DOI	10.1103/PhysRevB.84.214101
Self DOI	
URL	http://ir.lib.hiroshima-u.ac.jp/00034744
Right	(c) 2011 American Physical Society
Relation	

Off-center rattling and thermoelectric properties of type-II clathrate $(K, Ba)_{24}(Ga, Sn, \square)_{136}$ single crystals

S. Mano,[1] T. Onimaru,[1,*] S. Yamanaka,[2] and T. Takabatake[1,3]

[1]*Department of Quantum Matter, ADSM, Hiroshima University, Higashi-Hiroshima 739-8530, Japan*

[2]*Department of Applied Chemistry, Graduate School of Engineering, Hiroshima University, Higashi-Hiroshima 739-8527, Japan*

[3]*Institute for Advanced Materials Research, Hiroshima University, Higashi-Hiroshima, Hiroshima 739-8530, Japan*

(Received 4 October 2011; revised manuscript received 12 November 2011; published 6 December 2011)

We report the synthesis and temperature-dependent structural, transport, and thermal properties of type-II clathrate $K_{8+x}Ba_{16-x}Ga_{40-y}Sn_{96-z}\square_{y+z}$ ($1.2 \leqslant x \leqslant 2.8$, $2.0 \leqslant y \leqslant 3.3$, $0.8 \leqslant z \leqslant 6.6$, $\square$ = framework vacancy). Single-crystal x-ray diffraction analysis reveals that the guest K^+ and Ba^{2+} ions are preferentially incorporated into the hexakaidecahedral cages and dodecahedral cages, respectively. The guest site in the former splits into four sites 0.67 Å away from the center to the 32*e* site of the cage. The splitting is consistent with the presence of four minima in the electrostatic potential in the hexakaidecahedron. The thermopower is negative and relatively large, $-50 \sim -120$ μV/K at 300 K, indicating that the dominant charge carriers are electrons. The thermal conductivity displays a glasslike behavior with a plateau at around 20 K. The analysis of the specific heat indicates that the motion of the K^+ ion in the hexakaidecahedron can be described by the soft-potential model, including the tunneling term. The characteristic energy of 21 K for the soft mode is as low as that of the off-center rattling of the Ba^{2+} ion in type-I clathrate $Ba_8Ga_{16}Sn_{30}$. The present result on the type-II clathrate verifies the idea that the low-energy off-center rattling in oversized cages of intermetallic clathrates couples to the acoustic phonons to lead to the glasslike thermal conductivity.

DOI: 10.1103/PhysRevB.84.214101 PACS number(s): 72.15.Jf, 72.20.Pa, 82.75.−z

I. INTRODUCTION

Guest-framework compounds such as intermetallic clathrates and filled skutterudites have attracted much attention over the decades mainly due to their potential for thermoelectric materials.[1] Among intermetallic clathrates, type-I compounds with a formula A_8X_{46} and its subgroup $A_8E_{16}X_{30}$ (A = alkali metal, alkaline earth, and Eu; X = Si, Ge, and Sn) have been under intensive investigations.[2–7] The unit cell of type-I consists of 46 cage atoms arranged in two dodecahedra and six tetrakaidecahedra, which incorporate guest ions. In a Si clathrate $Na_2Ba_6Si_{46}$, the smaller guest ion Na^+ and the larger one Ba^{2+} are incorporated in the dodecahedron and tetrakaidecahedron, respectively.[8] When the mismatch between the guest ion size and the radius of the tetrakaidecahedron becomes large, as in $Eu_8Ga_{16}Ge_{30}$ and $Ba_8Ga_{16}Sn_{30}$, the guest ion occupies the off-center split sites away from the center. The off-center displacement of the split sites is approximately 0.4 Å in the two compounds.[4,5,9,10] The split sites are electrically stabilized by the charge distribution on the tetrakaidecahedral cage.[11] It has been revealed that the rattling of guest ions among the off-center sites couples with the lattice sound waves, leading to the glasslike thermal conductivity characterized by a plateau at low temperatures.[4,6,10]

Compared to type-I clathrates, less attention has been paid to the type-II clathrates, the unit cell of which consists of 8 hexakaidecahedra and 16 dodecahedra, as shown in Fig. 1(a).[12] The canonical example is Na_xSi_{136} ($0 \leqslant x \leqslant 24$), which was first reported in 1965 (Ref. 13), while the intrinsic transport properties have been revealed very recently.[14] Structural refinement of the crystal $Na_{22}Si_{136}$ indicated that Na ions in the Si_{28} cage are shifted off center.[15] The ternary derivatives of type-II can be written as $A_8E_{16}X_{136}$ (A and E = alkali metal; X = Si, Ge), where the cation A with relatively large radius is accommodated in the hexakaidecahedron and the cation E with relatively small radius is accommodated in the dodecahedron. $Cs_8Na_{16}Si_{136}$, $Cs_8Na_{16}Ge_{136}$ (Ref. 16), and $Ba_2Na_{16}Si_{136}$ (Ref. 17) exemplify the intercalation-type compounds, where the electrons released from the guest cations occupy the conduction-band states of Si_{136} and Ge_{136}.[14,18] Recently, Zintl-type compounds such as $Rb_{7.2}Na_{16}Ga_{20}Si_{116}$ and $Cs_8Na_{16}Ga_{21}Si_{115}$ have been synthesized,[19] where Ga atoms preferentially occupy the 96*g* site of the framework in Fig. 1(a). The alkaline-metal cation donates one electronic charge to Ga on the cage to form sp^3-like covalently bonded framework. In such Zintl-type compounds, the carrier density would be controlled by fine tuning the composition as successfully done in type-I clathrates.[20]

$Ba_{16}Ga_{32}Sn_{104}$ is the only Sn-based type-II clathrate reported so far.[21] Kröner and co-workers synthesized this compound by the reaction of a mixture of K:Ba:Ga:Sn in the ratio of 8:16:32:104. They reported neither elemental analysis nor physical properties, and concluded the lack of K atoms in the crystal solely from the structural analysis. Therefore, we have reinvestigated this compound as an extension of our studies of structural and thermoelectric properties of Sn-based clathrates $Ba_8Ga_{16}Sn_{30}$ and $K_8Ga_8Sn_{36}$.[9–11] We report herein the synthesis and temperature-dependent structural, transport, and thermal properties.

II. SINGLE-CRYSTAL GROWTH AND STRUCTURAL ANALYSIS

We have grown single crystals of $(K, Ba)_{24}(Ga, Sn)_{136}$ by the self-flux method using both Sn and Ga as flux. The starting compositions for three batches are listed in Table I. High-purity elements K, Ba, Ga, and Sn were loaded in a molybdenum crucible, which was subsequently sealed in a stainless-steel tube using Swagelok fittings. All manipulations were carried out inside a glove box under an argon atmosphere with water

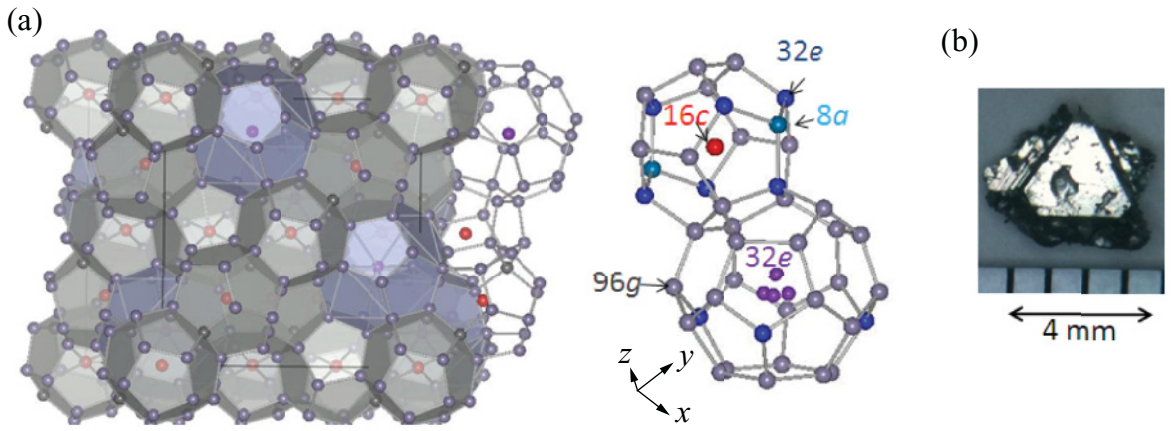

FIG. 1. (Color online) (a) Crystal structure of type-II clathrate composed of dodecahedron and hexakaidecahedron with guest atoms at the 16*c* and 32*e* split site, respectively. The cage atoms are at 8*a*, 32*e*, and 96*g* sites. (b) Photograph of a single crystal $K_{9.2}Ba_{14.8}Ga_{38.0}Sn_{95.2}\square_{2.8}$ grown by the Ga self-flux method.

concentration less than 0.06 ppm. The sealed tube was heated up to 550 °C, kept at 550 °C for 15 h, cooled at a rate of 1 °C/h to 450 °C. At this point, the tube was quickly removed from the furnace and the remaining molten flux was separated by centrifuging. The products were well-shaped crystals of 1–4 mm in diameter as shown in Fig. 1(b). The triangular faces are typical of compounds with a face-centered-cubic lattice.

Several crystals from each batch were crushed for powder x-ray diffraction measurements. The patterns with Cu $K\alpha$ radiation were recorded using a Rigaku Ultima IV diffractometer. The lattice parameters at 300 K for the three samples are in the range 17.063–17.079 Å, the values of which agree with 17.054 Å reported for $Ba_{16}Ga_{32}Sn_{104}$ at 293 K.[21] The crystal composition was determined by electron probe microanalysis (EPMA) using a JEOL JXA-8200 analyzer. The analysis revealed that the element K does exist in the crystals, which contradicts the previous report. Under the assumption that all cages are fully occupied, we estimated the compositions for three samples and listed the results in Table I. It is found that the guest compositions deviate from the ideal ratio 8:16 and the total number of Ga and Sn atoms is less than 136. The latter fact means the presence of vacancies on the cage site. Therefore, we describe the composition as $K_{8+x}Ba_{16-x}Ga_{40-y}Sn_{96-z}\square_{y+z}$ hereafter. The deviation from the ideal one 8:16:40:96 increases on going from #1 to #3. The melting point was determined by the differential thermal analysis (DTA) using BRUKER TG-DTA2000SA. The DTA curve recorded on heating at a rate of 5 °C/min exhibited an endothermic peak at 540 °C. The falloff point at 530 °C was taken as the melting point.

Single-crystal x-ray diffraction measurements were performed on crystals of 0.1 mm in diameter selected from the sample #1. We used a BRUKER APEXII ULTRA diffractometer with an imaging plate area detector using monochromatic Mo $K\alpha$ radiation ($\lambda = 0.710\,73$ Å). The data were recorded at various constant temperatures from 90 to 292 K. The crystal structure was refined using the WIN-GX software package.[22] We confirmed the cubic symmetry with the space group $Fd\bar{3}m$ (No. 227-2) and obtained the lattice parameter as 17.039(1) Å at 273 K. It should be noted that the hexakaidecahedral cage and dodecahedral cage preferentially accommodate the K^+ and Ba^{2+} ions, respectively. Thereby, the charge difference should be relevant because the ionic radii for the two ions are very similar in a high coordination environment: 1.64 Å for K^+ and 1.61 Å for Ba^{2+}.[23] The refined atomic coordinates, isotropic displacement parameters U_{eq}, and occupational parameters at 90 K are summarized in Table II. The final value of the reliability factor R (R_W) is 0.0153 (0.0215). In the refinement, the total number of vacancies on the cage was fixed to the value determined by EPMA. The probabilities of vacancies are determined to be 4% at the 32*e* site and 1.8% at the 96*g* site of the hexakaidecahedral cage, while the 8*a* site of the dodecahedral cage is fully occupied.

According to the structural analysis for $Na_{22}Si_{136}$,[15] the Na^+ guest in the hexakaidecahedron of the present system was assumed to occupy the 32*e* sites at $(3/8 + \delta, 3/8 + \delta, 3/8 + \delta)$ with $\delta = +0.016$. Similar analysis for

TABLE I. Starting composition, crystal composition, and lattice parameter *a* at 300 K for three samples of $K_{8+x}Ba_{16-x}Ga_{40-y}Sn_{96-z}\square_{y+z}$, where □ denotes the framework vacancy.

	Starting composition				Crystal composition					Lattice parameter
Batch No.	K	Ba	Ga	Sn	K	Ba	Ga	Sn	□	*a* (Å)
#1	8	16	47	96	9.2	14.8	38.0	95.2	2.8	17.063(3)
#2	8	16	40	108	10.1	13.9	37.2	95.0	3.9	17.079(3)
#3	8	16	45	108	10.8	13.2	36.7	89.4	9.9	17.079(1)

TABLE II. Atomic coordinates, occupational parameters, and isotropic displacement parameters U_{eq} of the sample #1 $K_{9.2}Ba_{14.8}Ga_{38.0}Sn_{95.2}\square_{2.8}$ at 90 K determined by single-crystal x-ray structure refinement.

Atom	Site	x	y	z	Occupational parameters	U_{eq} (Å^2) 90 K	173 K	273 K
K(1)/Ba(1)	32*e*	0.3521(7)	0.3521(7)	0.3521(7)	0.229(1)/0.021(1)	0.19(1)	0.20(1)	0.23(1)
K(2)/Ba(2)	16*c*	0	0	0	0.117(1)/0.882(1)	0.0127(2)	0.0188(2)	0.0260(1)
Ga(1)/Sn(1)	8*a*	0.125	0.125	0.125	0.425(3)/0.574(3)	0.00710(3)	0.0010(2)	0.0137(2)
Ga(2)/Sn(2)	32*e*	0.2185(2)	0.2185(2)	0.2185(2)	0.10(2)/0.86(1)	0.00890(2)	0.0120(1)	0.01641(1)
Ga(3)/Sn(3)	96*g*	0.0679(2)	0.0679(2)	0.3728(2)	0.326(6)/0.656(4)	0.0107(1)	0.0134(1)	0.0181(1)

$K_{9.2}Ba_{14.8}Ga_{38.0}Sn_{95.2}\square_{2.8}$ has led to the opposite sign of $\delta = -0.017$. The negative sign means that the 32*e* site of the guest shifts to the 32*e* site of the cage, as shown in Fig. 1(a). The displacement from the center at the 8*b* site is as large as 0.67 Å at 90 K. Figure 2 displays the difference Fourier maps of the charge density within the hexakaidecahedron viewed from the [001] direction. We obtained the differential intensity from the measured intensity by subtracting the intensity calculated for the hypothetical structure without the guest atom in the hexakaidecahedron. At 90 K, the charge density resides at four split sites, and the distribution changes to a toroidal shape with increasing temperature to 273 K.

We recall here that the guest site in the tetrakaidecahedron of type-I clathrate $Ba_8Ga_{16}Sn_{30}$ is split into four sites, which correspond to the four minima in the electrostatic potential created by Ga ions preferentially distributed on the three sites of the cage.[11] We expect an analogous situation in the hexakaidecahedron of type-II clathrate. We assumed that the Sn atom is electrically neutral, the Ga ion has a point charge of $-e$, and the vacancy at the 32*e* and 96*g* sites has the charge of $-4e$ as in the case of the Zintl compounds $Rb_8Sn_{44}\square_2$ and $Cs_8Sn_{44}\square_2$.[24–26] Then, the electrostatic potential is calculated as

$$\phi(r) = \sum_i \frac{1}{4\pi\epsilon_0}\frac{p_i q_i}{|r_i - r|} \quad , \tag{1}$$

where $\mathbf{r}_i$'s are the coordinates of the Ga atoms and vacancies, and q_i is $-e$ for the Ga ion and $-4e$ for the vacancy. With the use of the occupation probabilities p_i given in Table II, the potential was calculated in planes perpendicular to the z axis of the hexakaidecahedron (see Fig. 1). A clear double minimum appears as shown in Fig. 3 when the z coordinate with respect to the center was chosen as ± 0.2 Å. The geometry of the minima agrees with the 32*e* sites determined by the crystallographic analysis. However, the distance of 0.25 Å from the cage center to the minimum is shorter than 0.67 Å determined by crystallographic analysis. A possible reason for this disagreement will be discussed later.

The x-ray diffraction data at 173 and 273 K were also analyzed to determine the temperature dependences of the isotropic displacement parameters U_{eq}. Figure 4 shows the temperature dependences of U_{eq} for the guest atoms at 32*e* and 16*c* sites and cage atoms at three sites (see Fig. 1). Note that the U_{eq} for the 32*e* site is one order of magnitude larger than that for the 16*c* site. Assuming the guest Ba atom in the dodecahedron as an Einstein oscillator and the cage as a Debye solid, the parameters U_{eq} for the Ba atom and U_{eq} for the framework Ga/Sn atoms at a given temperature T are, respectively, written as

$$U_{eq}(\mathrm{Ba}) = \frac{\hbar^2}{2m_g k_B \theta_E}\coth\left(\frac{\theta_E}{2T}\right) + d^2, \tag{2}$$

$$U_{eq}(\mathrm{Ga/Sn}) = \frac{3\hbar^2 T}{m_{av} k_B \theta_D^2}\left[\frac{T}{\theta_D}\int_0^{\theta_D/T}\frac{x}{\exp(x)-1}dx + \frac{\theta_D}{4T}\right] + d^2, \tag{3}$$

where m_g, m_{av}, and d are mass of the guest atom Ba, the average mass of the framework atoms Ga/Sn, and temperature-independent disorder term, respectively.[7] As is shown in Fig. 4, the experimental data for the guest 16*c* site and the three cage sites can be fitted by using Eqs. (2) and (3), respectively. However, the data for the guest 32*e* site, which is preferentially occupied by the K atom, do not follow Eq. (2). The Einstein temperature derived from the fits to $U_{eq}(T)$ for the Ba atom at the 16*c* site is 69 K. The Debye temperatures of cage atoms are in the range from 188 to 199 K, which is comparable with the values reported for type-I $Ba_8Ga_{16}Sn_{30}$.[10]

III. TRANSPORT AND THERMAL PROPERTIES

We report here the measurements of the electrical resistivity ρ, thermopower S, thermal conductivity κ, and specific heat C on $K_{8+x}Ba_{16-x}Ga_{40-y}Sn_{96-z}\square_{y+z}$. The measurements of ρ and S were performed in the range from 4 to 300 K with homemade systems by a standard dc four-probe method and a differential method, respectively.[10] Figure 5 displays the data of $\rho(T)$ and $S(T)$ for three samples whose compositions are listed in Table I. For #1 with the composition most close to the ideal one, $\rho(T)$ shows a semiconducting behavior whereas $\rho(T)$ for #2 and #3 shows a metallic behavior. This trend is consistent with the decreasing of the absolute value of $S(T)$ from #1 to #3 and #2. In order to estimate the carrier density, the Hall coefficient R_H was measured on the sample #3 by a dc method in a field of 1 T applied by a conventional electromagnet. At 290 K, the measured R_H of -0.096 cm^3/C is consistent with the negative sign of S. If we assume one type carrier, electron charge carrier density is estimated as 6.5×10^{19}/cm^3 at 290 K. The dominant electron carriers contradict the expectation of hole conduction deduced from the Zintl concept, i.e., the guest K and Ba ions donate one and two electrons, respectively, and a vacancy on the cage accepts four electrons. The disagreement suggests the deviation in the valence balance from the strict Zintl counting

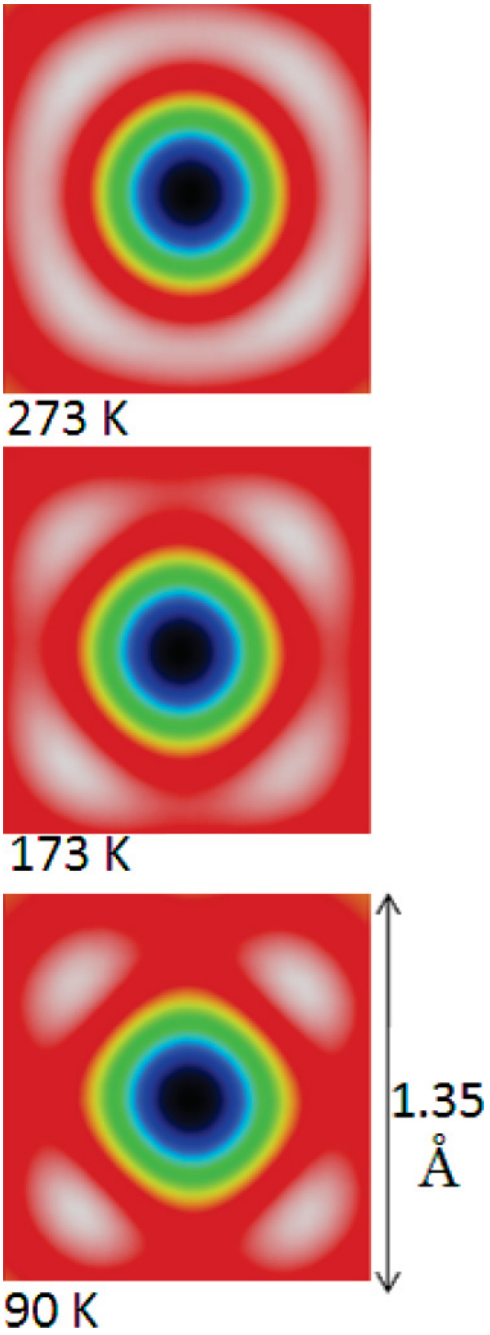

FIG. 2. (Color online) A (001) cross section of the differential Fourier map of the guest site in the hexakaidecahedral cage for $K_{9.2}Ba_{14.8}Ga_{38.0}Sn_{95.2}\square_{2.8}$ at three temperatures: 90, 173, and 273 K.

formalism.[27] This deviation may be responsible for the fact that the displacement of the split site determined from the structural refinement is larger than that calculated from the electrostatic potential.

The $\kappa(T)$ measurement was done on the sample #3 using a steady-state method in a range from 4 to 300 K. However, the effect of heat losses by radiation becomes serious in our measurement system at high temperatures above 150 K.[10] With decreasing temperature, $\kappa(T)$ monotonically decreases and exhibits no peak, as is shown in Fig. 6. The electronic contribution $\kappa_{el}(T)$ was estimated from the Wiedemann-Franz law $\kappa_{el}(T) = (\pi^2 k_B^2/3e^2)T/\rho(T)$ by using the measured $\rho(T)$ data. The $\kappa_{el}(T)$ and lattice contribution $\kappa_L(T) = \kappa(T) - \kappa_{el}(T)$ are displayed in Fig. 6. The data of $\kappa_L(T)$ for #3 are far low compared with those for type-I clathrate $K_8Ga_8Sn_{38}$ with on-center guests.[11] This contrasting result corroborates

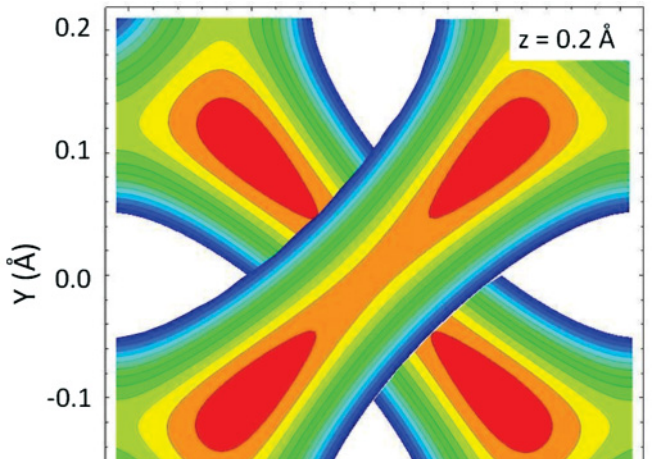

FIG. 3. (Color online) Electrostatic potential on two planes at $z = \pm 0.2$ in the hexakaidecahedron of $K_{9.2}Ba_{14.8}Ga_{38.0}Sn_{95.2}\square_{2.8}$, where the Ga ion and the vacancy on the cage were assumed to have point charges of $-e$ and $-4e$, respectively.

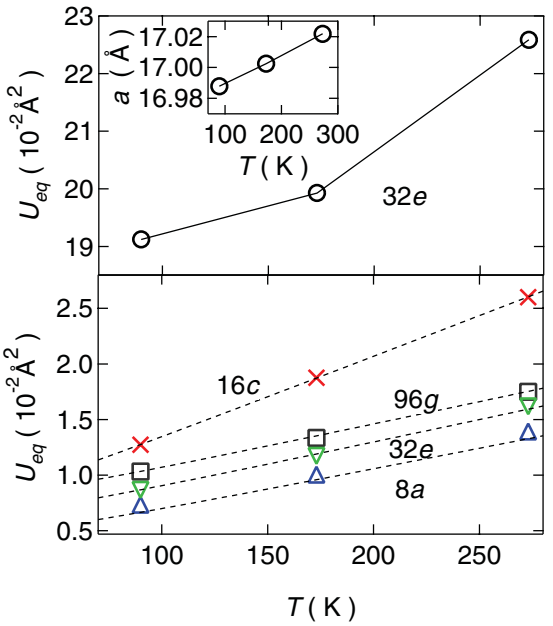

FIG. 4. (Color online) Temperature dependence of isotropic displacement parameters U_{eq} for guest atoms at the 16*c* and 32*e* split site and cage atoms at 8*a*, 32*e*, and 96*g* sites of $K_{9.2}Ba_{14.8}Ga_{38.0}Sn_{95.2}\square_{2.8}$. The dotted lines are the fits to the data using Eqs. (2) and (3), respectively. The inset shows the temperature dependence of lattice parameter.

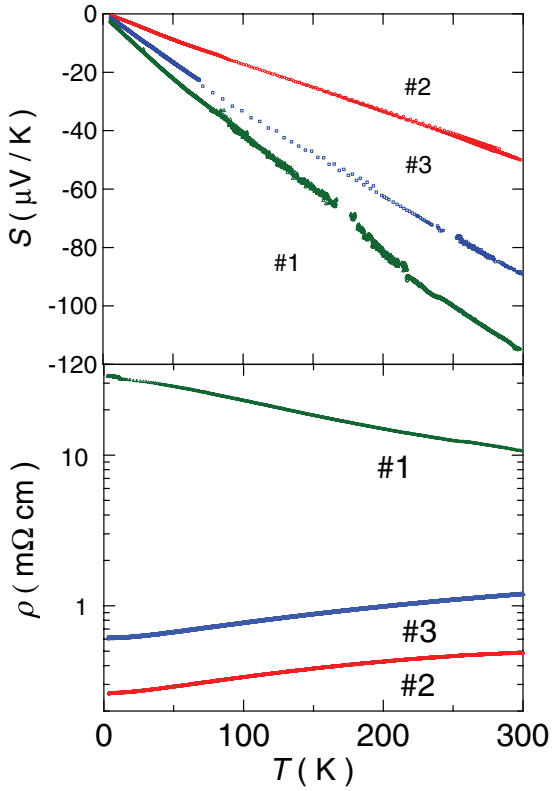

FIG. 5. (Color online) Temperature dependence of thermopower S and electrical resistivity ρ for three samples of $K_{8+x}Ba_{16-x}Ga_{40-y}Sn_{96-z}\square_{y+z}$.

the argument that off-center rattling is responsible for the suppression of $\kappa_L(T)$. Another mechanism to suppress $\kappa_L(T)$ is the scattering of acoustic phonons by the umklapp process, which should be enhanced in (K, Ba)$_{24}$(Ga, Sn,□)$_{136}$ with larger unit cell than $K_8Ga_8Sn_{38}$.[28] The vacancies on the cage framework may also suppress $\kappa_L(T)$. However, the scattering from vacancies and umklapp process do not explain why the data of $\kappa_L(T)$ for #3 are larger than those for the off-center rattling system $Ba_8Ga_{16}Sn_{30}$.[10] The lower $\kappa_L(T)$ in $Ba_8Ga_{16}Sn_{30}$ can be attributed the larger ratio of the off-center rattlers with respect to the number of all guest atoms. Note that the ratio of 6/8 for $Ba_8Ga_{16}Sn_{30}$ is twice larger than 8/24 for K_8Ba_{16}(Ga, Sn,□)$_{136}$.

Specific heat C of the sample #3 was measured from 0.5 to 300 K by a Quantum Design physical property measurement system using its standard thermal-relaxation method. Shown in Fig. 7 is the plot of C/T^3 versus T, where the contribution of the guest vibrations appears as a broad maximum over the Debye specific heat C_D of the cage atoms, which becomes constant at low temperatures. The Debye temperature was assumed to be equal to that obtained from the analysis of $U_{eq}(T)$ for the cage. The on-center guest vibration in the dodecahedron gives rise to Einstein specific heat C_E. The electronic term was assumed to be γT with $\gamma = 20$ mJ/K^2 mol that is derived from the electron charge carrier density 6.5×10^{19}/cm^3 using the free electron mode. Now, the remainder $C - C_D - C_E - \gamma T$ is the contribution of the off-center guest vibration in the hexakaidecahedron. To analyze this contribution, we use the soft-potential model (SPM) including the contributions of

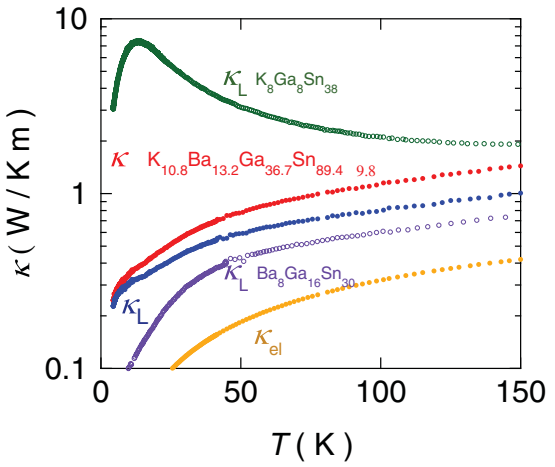

FIG. 6. (Color online) Temperature dependence of thermal conductivity κ, lattice part κ_L, and electrical part κ_{el} for $K_{10.8}Ba_{13.2}Ga_{36.7}Sn_{89.4}\square_{9.8}$. The data of κ_L for type-I clathrates $K_8Ga_8Sn_{38}$ and $Ba_8Ga_{16}Sn_{30}$ are taken from Refs. 10 and 11, respectively.

tunneling two-level systems (TS).[29] Because the tunneling term is proportional to T, it is not distinguished from the electronic term. However, the plot of C/T versus T^2 has an intercept of 98 mJ/K^2 mol, which is five times larger than $\gamma =$ 20 mJ/K^2 mol. Therefore, the most part of the T-linear term is ascribed to the tunneling contribution.

The soft-potential model explained the broad maximum in C/T^3 and the upturn at low temperatures for off-center rattling clathrates such as $Ba_8Ga_{16}Sn_{30}$ and $Sr_8Ga_{16}Ge_{30}$.[10,30] The details of equations and notations are described in Ref. 30.

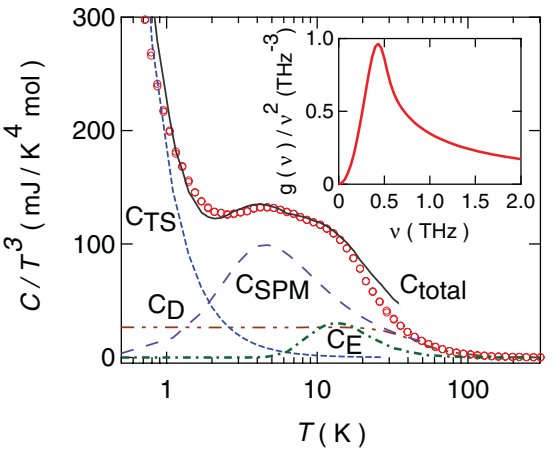

FIG. 7. (Color online) Temperature dependence of specific heat presented as C/T^3 vs T for $K_{10.8}Ba_{13.2}Ga_{36.7}Sn_{89.4}\square_{9.8}$ (open circles), C_E (dashed-dotted line), and C_D (dashed and double-dotted line), respectively, represent the calculations of the Einstein contribution of the guest vibration in the dodecahedron and the Debye contribution of the cages. C_{SPM} (long-dashed line) and C_{TS} (short-dashed line) denote the soft-mode and tunneling contributions of the guest vibration in the hexakaidecahedron. C_{total} denotes the sum of all the contributions, including the electronic contribution. The inset shows the soft-mode vibration density of states $g(\nu)/\nu^2$ as a function of the frequency ν (see text).

In Fig. 7, the two contributions C_{SPM} and C_{TS} are represented by the long-broken line and the short-broken line, respectively, and the sum of all contributions C_{total} is drawn by the solid line. The parameters to describe C_{SPM} and C_{TS} are the characteristic energy of the potential $W/k_B = 4.7$ K, the distribution constant of soft potential $P_s = 2.7 \times 10^{22}$/mol, and the coefficient of the distribution $A = 0.05$. Using these parameters, the soft vibrational density of states g as a function of the frequency ν was calculated. The inset of Fig. 7 shows the profile of $g(\nu)/\nu^2$ with a peak at 0.43 THz, the energy of which corresponds to 21 K. This characteristic energy is as low as that of the off-center rattling in type-I $Ba_8Ga_{16}Sn_{30}$.

IV. SUMMARY

We have synthesized single crystals of type-II clathrate $K_{8+x}Ba_{16-x}Ga_{40-y}Sn_{96-z}\square_{y+z}$ ($1.2 \leqslant x \leqslant 2.8$, $2.0 \leqslant y \leqslant 3.3$, $0.8 \leqslant z \leqslant 6.6$, $\square$ = framework vacancy), and studied the structural and thermoelectric properties at low temperatures. This compound is found to be a rare example of type-II clathrate, which can be classified into Zintl phases. Structural refinement revealed that the K^+ and Ba^{2+} with comparable ionic radii are preferentially incorporated into the hexakaidecahedral cage and dodecahedral cage, respectively. Furthermore, the guest site in the hexakaidecahedral cage split into four sites 0.67 Å away from the center to the 32*e* site of the cage. The calculation of the electrostatic potential in the hexakaidecahedron revealed four minima at the same geometric sites as the split sites, indicating that the split sites are stabilized by the electrostatic potential. The contribution of the guest motion in the hexakaidecahedron to the specific heat can be described by the soft-potential model, including the tunneling term. The characteristic energy of 21 K for the off-center rattling is as low as that in the typical phonon-glass clathrate $Ba_8Ga_{16}Sn_{30}$. Thus, glasslike behavior in the lattice thermal conductivity in both type-II clathrate $K_{8+x}Ba_{16-x}Ga_{40-y}Sn_{96-z}\square_{y+z}$ and type-I $Ba_8Ga_{16}Sn_{30}$ confirms that the coupling of low-energy off-center rattling to acoustic phonons plays the central role in the glasslike thermal conductivity at low temperatures.

ACKNOWLEDGMENTS

We would like to thank K. Suekuni and K. Umeo for useful discussions. We thank T. Mizuta for his help in the single-crystal x-ray diffraction measurement. Y. Shibata is appreciated by the EPMA performed at Natural Science Center for Basic Research and Development, Hiroshima University. This work was supported by NEDO of Japan under Grant No. 09002139-0 and by MEXT of Japan under Grant-in-Aid for Scientific Research, Grants No. 19051011 and No. 20102004.

*onimaru@hiroshima-u.ac.jp

[1] For a recent review, see *Thermoelectrics Handbook Macro to Nano*, edited by D. M. Rowe (Taylor & Francis, Boca Raton, 2006).
[2] G. S. Nolas, J. L. Cohn, G. A. Slack, and S. B. Schujman, Appl. Phys. Lett. **73**, 178 (1998).
[3] S. Paschen, W. Carrillo-Cabrera, A. Bentien, V. H. Tran, M. Baenitz, Yu. Grin, and F. Steglich, Phys. Rev. B **64**, 214404 (2001).
[4] B. C. Sales, B. C. Chakoumakos, R. Jin, J. R. Thompson, and D. Mandrus, Phys. Rev. B **63**, 245113 (2001).
[5] B. C. Chakoumakos, B. C. Sales, and D. G. Mandrus, J. Alloys Compd. **322**, 127 (2001).
[6] F. Bridges and L. Downward, Phys. Rev. B **70**, 140201(R) (2004).
[7] A. Bentien, E. Nishibori, S. Paschen, and B. B. Iversen, Phys. Rev. B **71**, 144107 (2005).
[8] S. Yamanaka, H. Horie, H. Nakano, and M. Ishikawa, Fullerene Sci. Technol. **3**, 21 (1995).
[9] M. A. Avila, K. Suekuni, K. Umeo, H. Fukuoka, S. Yamanaka, and T. Takabatake, Appl. Phys. Lett. **92**, 041901 (2008).
[10] K. Suekuni, M. A. Avila, K. Umeo, H. Fukuoka, S. Yamanaka, T. Nakagawa, and T. Takabatake, Phys. Rev. B **77**, 235119 (2008).
[11] T. Tanaka, T. Onimaru, K. Suekuni, S. Mano, H. Fukuoka, S. Yamanaka, and T. Takabatake, Phys. Rev. B **81**, 16510 (2010).
[12] M. Beekman and G. S. Nolas, J. Mater. Chem. **18**, 842 (2008), and references therein.
[13] J. S. Kasper, P. Hagenmullar, M. Pouchard, and C. Cros, Science **150**, 1713 (1965).
[14] M. Beekman, W. Schnelle, H. Borrmann, M. Baitinger, Yu. Brin, and C. S. Nolas, Phys. Rev. Lett. **104**, 018301 (2010).
[15] M. Beekman, C. P. Sebastian, Yu Grin, and G. S. Nolas, J. Electron. Mater. **38**, 1136 (2009).
[16] S. Bobev and S. C. Sevov, J. Am. Chem. Soc. **121**, 3795 (1999).
[17] T. Rachi, K. Tanigaki, R. Kumashiro, J. Winter, and H. Kuzmany, Chem. Phys. Lett. **409**, 48 (2005).
[18] K. Biswas and C. W. Myles, Phys. Rev. B **74**, 115113 (2006).
[19] S. Bobev, J. Meyers Jr., V. Fritsch, and Y. Yamasaki, in *Proceedings of the 25th International Conference on Thermoelectrics* (IEEE catalog No. 06TH8931, Piscataway, NJ, 2006), p. 48.
[20] M. A. Avila, K. Suekuni, K. Umeo, H. Fukuoka, S. Yamanaka, and T. Takabatake, Phys. Rev. B **74**, 125109 (2006).
[21] R. Kröner, K. Perters, H. G. von Schnering, and R. Nesper, Z. Kristallogr. New Cryst. Struct. **213**, 664 (1998).
[22] L. J. Farrugia, J. Appl. Crystallogr. **32**, 837 (1999).
[23] R. D. Shannon, Acta Crystallogr., Sect. A: Cryst. Phys., Diffr., Theor. Gen. Crystallogr. **32**, 751 (1976).
[24] J. T. Zhao and J. D. Corbett, Inorg. Chem. **33**, 5721 (1994).
[25] G. S. Nolas, B. C. Chakoumakos, B. Mahieu, G. J. Long, and T. J. R. Weakley, Chem. Mater. **12**, 1947 (2000).
[26] F. Dubois and T. F. Fässler, J. Am. Chem. Soc. **127**, 3264 (2005).
[27] S. M. Kauzlarich, S. R. Brown, and G. J. Snyder, Dalton Trans. **21**, 2099 (2007).
[28] J. Yang, in *Thermal Conductivity: Theory, Properties, and Applications*, edited by T. M. Tritt (Kluwer Academic, New York, 2004), p. 1.
[29] M. A. Ramos and U. Buchenau, in *Tunneling Systems in Amorphous and Crystalline Solids*, edited by P. Esquinazi (Springer, Berlin, 1998), Chap. 9, p. 527.
[30] K. Umeo, M. A. Avila, T. Sakata, K. Suekuni, and T. Takabatake, J. Phys. Soc. Jpn. **74**, 2145 (2005).